Geophysical Research Letters

RESEARCH LETTER
10.1029/2019GL083776

The 2005 Amazon Drought Legacy Effect Delayed the 2006 Wet Season Onset

Mingjie Shi[1,2], Junjie Liu[1,3], John R. Worden[1], A. Anthony Bloom[1], Sun Wong[1], and Rong Fu[2]

[1]Jet Propulsion Laboratory, California Institute of Technology, Pasadena, CA, USA, [2]Joint Institute for Regional Earth System Science and Engineering, Department of Atmospheric and Oceanic Sciences, University of California, Los Angeles, CA, USA, [3]Division of Geological and Planetary Sciences, California Institute of Technology, Pasadena, CA, USA

Abstract While the long-term drought effect on tropical forests has been observed in ground-based and remote sensing measurements, the feedback of reduced forest biomass on subsequent rainfall is not well understood. We evaluate the impact of slow forest recovery after the 2005 Amazonian drought on local evapotranspiration (ET) and wet season onset (WSO) using remotely sensed precipitation, deuterium retrievals, reanalysis data, and a new ET product. A comparison to the 2009 rainy season, which exhibits similar large-scale moisture flux convergence, shows that 2006 experienced a 25% ET reduction and 20 days of postponed WSO in the dry-to-wet transition. Our results imply that ET reduction due to drought-driven legacy effect on the Amazon rainforest could be a crucial factor triggering WSO delay in the transitional season following drought events.

Plain Language Summary Drought legacy effect, observed as reduced growth and incomplete forest recovery after severe drought events, impacts the carbon and water cycles of Amazonia. Satellite observations showed a reduction of canopy carbon during and after the 2005 Amazonian drought. To understand the impact of local evapotranspiration (ET) changes associated with this canopy carbon reduction on the timing of wet season onset (WSO) over southern Amazonia, we study the precipitation and ET changes in the 2006 dry-to-wet transition by using space-based remote sensing of precipitation, deuterium retrievals, reanalysis data, and a new ET product. A comparison to the 2009 rainy season, which has a similar large-scale moisture flux convergence amount, shows a 25% reduction in ET and 20 days of postponed WSO during the dry-to-wet transition of 2006. Our results indicate that drought legacy effects could be a crucial factor triggering WSO delay following drought events and imply the importance of accurately representing biogeochemical processes and land-atmosphere feedbacks when predicting precipitation over Amazon in Earth system models.

Key Points:
- Precipitation observations from TRMM show a postponed wet season onset in southern Amazonia in 2006
- Both deuterium retrievals from TES and a new evapotranspiration (ET) product suggest an ET reduction during the late transition of 2006
- ET reduction due to 2005 Amazonian drought legacy effect on forest delays the wet season onset in 2006

Supporting Information:
- Supporting Information S1

Correspondence to:
M. Shi,
mingjie.shi@jpl.nasa.gov

Citation:
Shi, M., Liu, J., Worden, J. R., Bloom, A. A., Wong, S., & Fu, R. (2019). The 2005 Amazon drought legacy effect delayed the 2006 wet season onset. *Geophysical Research Letters*, *46*, 9082–9090. https://doi.org/10.1029/2019GL083776

Received 21 MAY 2019
Accepted 8 JUL 2019
Accepted article online 15 JUL 2019
Published online 9 AUG 2019

1. Introduction

Amazonian forests have substantial influence on regional and global climate (Gedney & Valdes, 2000; Nobre et al., 1991). Across the Amazon, 25% to 70% of rainfall is recycled through evapotranspiration (ET; Eltahir & Bras, 1994; Malhi et al., 2008; Salati & Vose, 1979). ET is especially crucial during the initial stage of the dry-to-wet transition, since it moistens and destabilizes the atmosphere (Wright et al., 2017). Consequently, forest loss from drought could cause reduced rainfall and delayed wet season onset (WSO).

Modeling studies have shown that drought and Amazonian forest loss may amplify each other. Specifically, the forest loss intensifies regional droughts (Betts et al., 2004; Dickinson & Kennedy, 1992; Zemp et al., 2017) as a result of the reduced dry-season forest transpiration. Intensified drought events further inhibit forest recovery (Poorter et al., 2016; Verbesselt et al., 2016) through increased mortality and likelihood of fire (Brando et al., 2014). Some Earth system models that incorporate this feedback between drought and forest loss have predicted an increase of drought severity and dry season length (DSL; Aragão et al., 2014; Duffy et al., 2015; Li et al., 2006) and conversions of tropical forest to a lower tree cover ecosystem (Hirota et al., 2011; Oyama & Nobre, 2003; Staver et al., 2011; Xu et al., 2016).

Recent observations of precipitation and ET have begun to support this modeling evidence. Fu et al. (2013) show that the DSL increased by 1.3 ± 0.5 pentads (5 days) per decade over the southern Amazon during 1979–2011, primarily through delayed WSO. Wright et al. (2017) show that during the dry season the

local ET triggers the WSO over the southern Amazon, implying that the reduction of ET during the dry season could delay WSO. Saatchi et al. (2013) and Shi et al. (2017) show with observations and modeling, respectively, that the forest loss from 2005 Amazonian drought persisted for about 3 years, which implies a reduction of local ET and a possible delay of WSO following this drought. Here we use observations to investigate whether forest loss resulted from the 2005 drought reduces ET in 2006 and delays 2006 WSO. Our study provides observational evidence on whether it is possible to have self-amplified drought through land-atmosphere feedbacks.

2. Method

2.1. Precipitation Data and WSO Definition

The observed WSO is characterized with precipitation measurements from the Tropical Rainfall Measuring Mission (TRMM) 3B42 (1997–2015; Huffman et al., 2007), provided at 0.25° × 0.25° and 3-hourly *spatiotemporal* resolutions. The daily precipitation rates, integrated from the 3-hourly TRMM precipitation rate, is averaged over a 5-day period (pentad). The observed WSO is defined as the first pentad when the mean pentad precipitation rate exceeds the climatological annual mean precipitation rate during six out of eight pentads (Fu et al., 2013). Here the first pentad of WSO is defined as pentad 0, and the pentads before WSO are labeled negatively and vice versa.

2.2. Large-Scale Moisture Flux Convergence

Precipitation has two main sources: large-scale moisture flux convergence (equation (1)) and local ET. Here we use European Centre for Medium Range Weather Forecasts Re-Analysis (ERA)-Interim, provided at 0.7° × 0.7° and 3-hourly *spatiotemporal* resolutions, to calculate the atmospheric large-scale moisture flux convergence as (Wong et al., 2016)

$$P-E+\frac{\partial Q}{\partial t}=-\nabla\cdot\mathbf{F}, \tag{1}$$

where

$$Q(x,y,t)=\int_{ptop}^{psrf}q(x,y,p,t)\frac{dp}{g} \tag{2}$$

and

$$\mathbf{F}(x,y,t)=\int_{ptop}^{psrf}q(x,y,p,t)\mathbf{v}(x,y,p,t)\frac{dp}{g}, \tag{3}$$

where P is precipitation, E is surface evaporation, and Q and $\mathbf{F}$ are column-integrated specific humidity q (SPHU) and moisture flux, respectively, from the top of the atmosphere (*ptop*, at 0.1 hPa) to the surface (*psrf*). The vector $\mathbf{v}$ is horizontal winds. Here x and y represent longitude and latitude, respectively; p represents pressure levels; and t represents time. The tendency of Q, $\frac{\partial Q}{\partial t}$, is much smaller than the other terms after temporal and regional averages and can be ignored. Therefore, the change of precipitation is the result of changes in E and $-\nabla\cdot\mathbf{F}$. We name $-\nabla\cdot\mathbf{F}$ as Q_{ATMO}.

The increase of water vapor from large-scale moisture flux convergence and/or local ET during the late transition season (i.e., −6–0 pentad) is a precondition for the WSO (Wright et al., 2017). To isolate the impact of drought-driven ET anomalies on WSO, we first identify the baseline years that have $Q_{\mathrm{ATMO,year}}$ within ±1 standard deviation (σ) of $Q_{\mathrm{ATMO,2006}}$ during the −6–0 pentad before the climatological WSO. Q_{ATMO} in each year is calculated as

$$Q_{\mathrm{ATMO,year}}=\sum_{i=-6}^{0}Q_{\mathrm{ATMO}}, \tag{4}$$

where i is the pentad number before WSO.

2.3. A New ET Product

By following the ET estimation approach from Swann and Koven (2017) and Maeda et al. (2017), monthly total ET across watersheds in the Amazon is derived from satellite observations of precipitation and terrestrial water storage (TWS) and ground-based measurements of river runoff. Unlike the ET retrievals from the Moderate Resolution Imaging Spectroradiometer, which have been shown to be seasonally biased in the wet tropics (Maeda et al., 2017; Swann & Koven, 2017), this ET estimation is robust across seasons (Swann & Koven, 2017). To keep the consistency between the precipitation used to identify WSO and that used to estimate ET, we use TRMM precipitation in deriving ET. We use three Gravity Recovery and Climate Experiment (GRACE) TWS retrievals from Center for Space Research, GeoforschungsZentrum Potsdam, and Jet Propulsion Laboratory (JPL) and calculate the arithmetic mean of these GRACE TWS retrievals (Sakumura et al., 2014). Runoff data sets for each watershed are obtained from the Observation Service for the geodynamical, hydrological, and biogeochemical control of erosion/alteration and material transport in the Amazon, Orinoco, and Congo basins (SO-HYBAM) in situ river gauge discharge measurements spanning 2003–2015 (Figure 1a). With these three data sets, we estimate subbasin-based monthly ET (herein ET_{OBS}; Text S1 in the supporting information).

ET_{OBS} uncertainty estimates (σ_{ET}) are from three components: precipitation (σ_{RAIN}), GRACE (σ_{GRACE}), and runoff (σ_{RUNOFF}). Besides TRMM, we use the Precipitation Estimation from Remotely Sensed Information derived from Artificial Neural Networks (PERSIANN) product ($0.25° \times 0.25°$ and daily *temporal* resolutions; Ashouri et al., 2015) and the Climate Research Unit (CRU) version 4 ($0.5° \times 0.5°$ and monthly *spatiotemporal* resolutions; New et al., 2000) to identify σ_{RAIN}. The monthly GRACE TWS uncertainty is estimated to be 25 mm for an 800-km averaging radius (Rodell et al., 2004), approximately the same size of the selected basin groups (Figure 1a). Thus, σ_{GRACE} is 25 mm. We are not aware of any monthly runoff uncertainty estimates; we acknowledge that these are unaccounted for in our ET estimates. We assume σ_{RUNOFF} is 10% of the runoff amount in each Amazonian subbasin. Thus, σ_{ET} is estimated as

$$\sigma_{ET} = \sqrt{\sigma_{RAIN}^2 + \sigma_{GRACE}^2 + \sigma_{RUNOFF}^2}. \quad (5)$$

2.4. The Criteria of Study Case Selection

We have three criteria to select the study region: (1) regions with mean evergreen tropical forest cover ≥50%, (2) regions that can find baseline years with similar Q_{ATMO} values to that in the year after drought (equation (6)), and (3) regions that have consistent precipitation variability between basin area-weighted mean (herein $TRMM_{basin}$) and the mean of the regular regions overlapping with the basins (herein $TRMM_{region}$) during late transition. The climatology is defined as 2001–2015.

The calculations of large-scale moisture flux convergence and local ET in different subregions show that Q_{ATMO} has much larger interannual variability than local ET (Tables S1 and S2). Thus, a "similar Q_{ATMO} year" is defined as

$$\left|Q_{ATMO,year} - Q_{ATMO,2006}\right| \le \sigma_{ET,baseline}, \quad (6)$$

where $Q_{ATMO,year}$ is the Q_{ATMO} values during the −6–0 pentad in a specific year, $Q_{ATMO,2006}$ is the Q_{ATMO} in 2006, and $\sigma_{ET,\ baseline}$ is the interannual variability of ET_{OBS} between the baseline years. Thus, we select years with similar Q_{ATMO} as that of the first year after drought to address the impact of drought-induced ET reduction on WSO. Since ET_{OBS} is based on different Amazonia river basins, which are irregular, having consistent precipitation variabilities between $TRMM_{basin}$ and $TRMM_{region}$ is also a criterion.

2.5. Water Isotope Observations and the Theoretical Model

To provide evidence of differences in moisture source after drought, we use SPHU and δD retrievals (October 2004 to March 2011) from the Tropospheric Emission Spectrometer (TES) onboard the Aura satellite (Worden et al., 2006). δD is calculated as

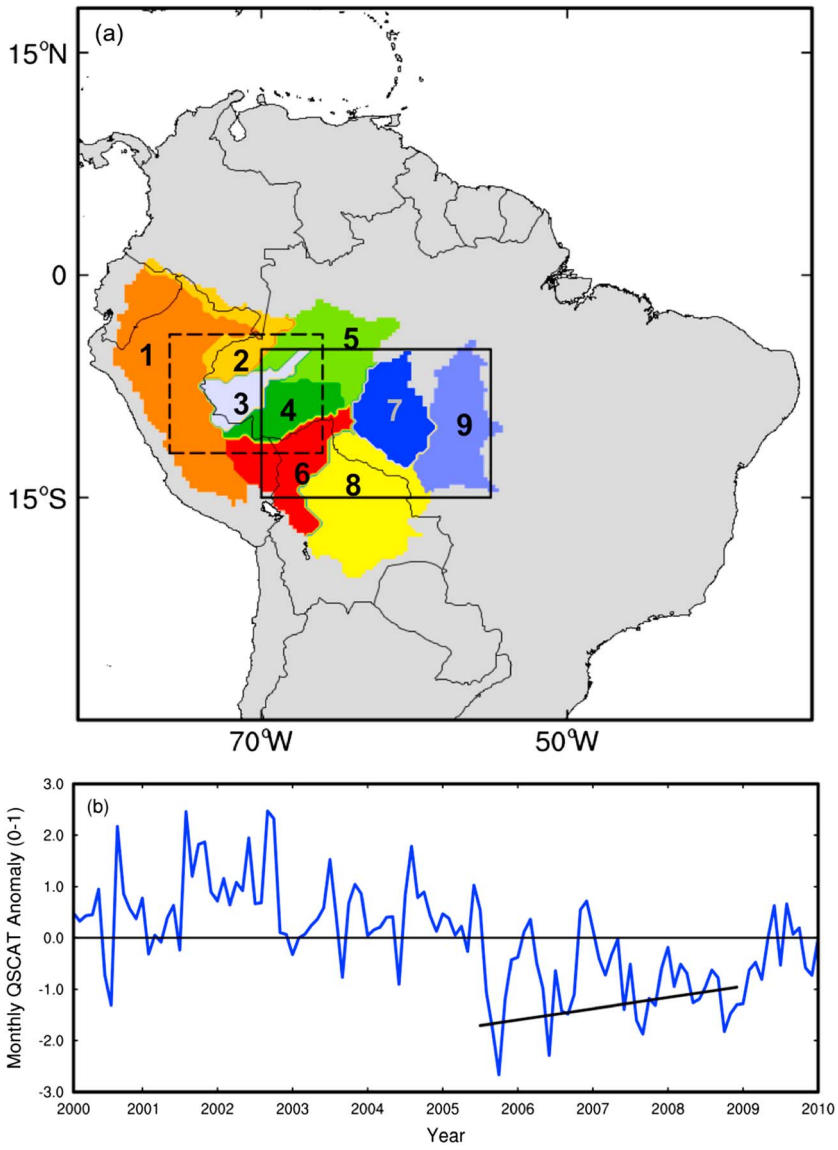

Figure 1. (a) The watershed distribution map of ET_{OBS}. The dashed box represents 4–12°S, 66–76°W, and the solid box represents 5–15°S, 55–70°W. (b) The SeaWinds Scatterometer onboard QuikSCAT backscatter anomaly over 5–15°S, 70–55°W and the regression line (black) during July 2005 to October 2008.

$$\delta D = 1,000 \times \left(\frac{R - R_{\text{std}}}{R_{\text{std}}} \right), \tag{7}$$

where R is the ratio of the number of HDO molecules (N_{HDO}) to the number of $H_2{}^{16}O$ molecules (N_{H2O}). R_{std} is the corresponding N_{HDO}/N_{H2O} ratio in a reference standard; here we use the Vienna Standard Mean Ocean Water, for which $R_{std} = 3.11 \times 10^{-4}$. Over the southern Amazon, the typical uncertainties of TES retrievals are ~7–10% for SPHU and ~3–5% for R in the free troposphere (750–348 hPa). The mean degrees of freedom of HDO/H_2O retrievals in the vertical layers are ~0.5–0.6 at the top of the atmospheric boundary layer (surface to 825 hPa) and ~1.2–1.6 in the free troposphere (750–348 hPa). Thus, these data can distinguish TES δD-SPHU variations in both the atmospheric boundary layer and free troposphere (Wright et al., 2017). The TES SPHU and δD retrievals have limited sampling after March 2011 due to instrument aging.

We use a theoretical rainfall (Rayleigh) and atmospheric mixing model to group the moisture sources: water vapor transpired from the forest and water vapor evaporated from the ocean (e.g., Galewsky et al., 2016;

Noone et al., 2011; Worden et al., 2006). δD evaporated under thermodynamic equilibrium conditions from the tropical ocean has an isotopic composition of approximately −70‰ to −90‰, while it is approximately 0 to −60‰ for rainforest ET (Risi et al., 2013; Wright et al., 2017). Thus, oceanic evaporation and tropical forest ET are isotopically distinct moisture sources, with forest ET relatively enriched in deuterium (Worden et al., 2006; Wright et al., 2017).

Sampling variations of satellite observations could cause changes in the physical quantities they observe. TES HDO/H_2O observations have a similar sampling density in the late transition of 2005–2009 in our study region, with the sampling numbers 105, 94, 99, 106, and 103, respectively. Thus, the TES HDO/H_2O interannual variability does not come from sampling variability. Besides the impacts from oceanic evaporation and local ET, strong subsidence could also be a reason for isotopic depletion (Brown et al., 2008). Thus, we use the 500-hPa vertical velocity from ERA-Interim to identify subsidence.

3. Results

3.1. Study Region Selection

We first investigate two Amazonian subregions: western Amazonia (4–12°S, 66–76°W; Saatchi et al., 2013) and southern Amazonia (5–15°S, 50–70°W; Li & Fu, 2004). Evergreen tropical forest has a 38% coverage in 5–15°S, 50–55° W, while it is 73% over 5–15°S, 55–70°W (Figure S2). Thus, we narrow down the research area to 5–15°S, 55–70°W (the first criterion). We then apply the second criterion to the western Amazon and narrowed southern Amazon; 2005, 2010, and 2015 are drought years over the Amazon (Table S3); thus, we exclude these 3 years for the calculation. We study ET_{OBS} in September, October, and November (SON), during which the wet season usually has its onset in the Amazon (Table S1).

In western Amazonia, $Q_{ATMO,2006}$ is 20 mm/month, and Q_{ATMO} in 2003 (54 mm/month), 2004 (52 mm/month), 2009 (5 mm/month), 2011(53 mm/month), and 2013 (48 mm/month) is within $\pm 1\sigma$ of $Q_{ATMO,2006}$. However, the standard deviation of SON ET_{OBS} over basins 2, 3, and 4 (Figure 1a) in these selected 5 years is 12 mm/month. Not a single year of these 5 years has a Q_{ATMO} value between $Q_{ATMO,2006} \pm \sigma_{ET,\ baseline} = 20 \pm 12\ \text{month}^{-1}$ (Table S1). Thus, western Amazonia is excluded by the second criterion (Text S3).

In the narrowed southern Amazonia, the years 2003, 2004, 2007, 2008, 2009, and 2014 are identified within $\pm 1\sigma$ of $Q_{ATMO,2006}$. The spatially weighted mean ET_{OBS} over basins 4, 6, 7, and 9 (Figure 1a), covering 66% of 5–15°S, 55–70°W, has standard deviation of 8 mm/month among these 6 years. Using the second criterion, we find 2009 (Q_{ATMO} = 30 mm/month) has Q_{ATMO} satisfy equation (6) ($Q_{ATMO,2006} \pm \sigma_{ET,baseline} = 32 \pm 8$ mm/month; Table 1). In addition, $TRMM_{basin}$ and $TRMM_{region}$ have consistent variability in September and October between these 2 years (Figure S4). Thus, we investigate the impact of drought-induced ET reduction on WSO in 5–15°S, 55–70°W and define 2009 as a "similar Q_{ATMO} year" (Text S3).

3.2. ET_{OBS} Reduction in 2006

The ET_{OBS} anomaly over 5–15°S, 55–70°W is −64, −51, and 50 mm/year in 2005, 2006, and 2007, respectively. ET_{OBS} is 87 ± 27, 100 ± 28, and 92 ± 26 mm/month in SON of 2006, respectively, while the mean ET_{OBS} values over the baseline years (Table 1) is 108 ± 27, 120 ± 27, and 115 ± 26 mm/month in the same 3 months (Figure 2). We also calculate ET with each individual GRACE TWS product. During 2006 SON, the 3-month mean ET_{OBS} anomaly from any of these products is negative (the mean is −20 mm/month), lower than the SON mean ET_{OBS} anomaly (2 mm/month) over the baseline years (Table S5). Thus, all three ET_{OBS} from TRMM + GRACE retrievals give similar results with respect to the comparison between SON ET_{OBS} in 2006 and those values over the six baseline years. Compared to the mean ET_{OBS} in the baseline years, the 2006 ET_{OBS} decreases by 18% (Table 1), suggesting that the observed drought legacy effect on evergreen tropical trees (Figure 1b) may have led to an ET reduction in 2006. Note that ET_{OBS} has negative anomaly values −103, −41, −7, and −42 mm/year in basins 4, 6, 7, and 9 in 2006, respectively, corresponding to the radar backscatter signal in 2006 (Text S2 and Figure 1b) and precipitation anomaly in 2005 (Figure S1a).

Q_{ATMO} has larger interannual variability ($\sigma_{2001–2015}$ = 33.0 mm/month) than ET_{OBS} ($\sigma_{2003–2015}$ = 9 mm/month), and the Q_{ATMO} difference between 2006 and the baseline years ranges from −100% (in 2008) to 72% (in 2014). To further isolate the impact of ET from Q_{ATMO}, we compare 2006 to 2009 since the late

Table 1
Q_{ATMO} During the Late Transition Obtained From European Centre for Medium-Range Weather Forecasts-Interim, the Area-Averaged ET_{OBS} Over SON, and Tropical Rainfall Measuring Mission Suggested WSO in 2003, 2004, 2006, 2007, 2008, 2009, and 2014

Year	Q_{ATMO} (mm/month)	Mean of SON ET_{OBS} (mm/month)	Pentad of WSO
2006	32	93.0	64
2003	21	111	66
2004	22	112	64
2007	48	110	58
2008	0	124	66
2009	30	124	60
2014	55	104	61
Mean of the baseline years	30 ± 20	114 ± 8	63 ± 3

Note. Q_{ATMO} = large-scale moisture flux convergence; ET = evapotranspiration; SON = September, October, and November; WSO = wet season onset.

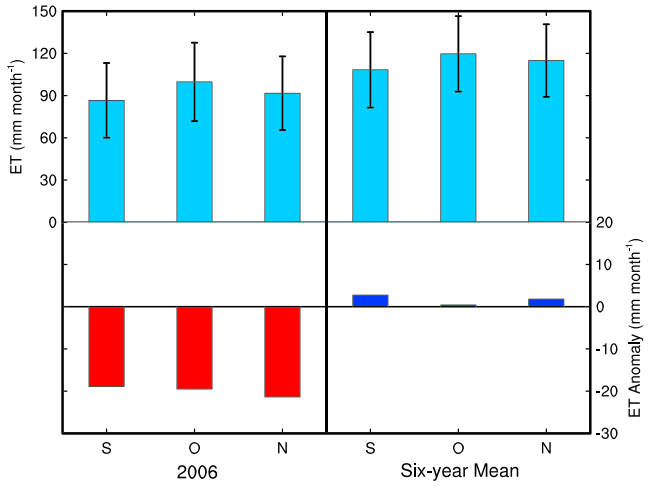

Figure 2. Area-averaged ET_{OBS} (upper) and ET_{OBS} anomaly (lower) over watersheds 4, 6, 7, and 9 in September (S), October (O), and November (N) of 2006 and the mean of these two variables over the baseline years (2003, 2004, 2007, 2008, 2009, and 2014). The error bar is σ_{ET}. ET = evapotranspiration.

transition Q_{ATMO} difference between 2006 and 2009 is 2 mm/month less than $\sigma_{ET,baseline}$ (Table 1). Compared to 2009, the SON ET_{OBS} in 2006 has a 25% reduction. Meanwhile, 2009 WSO is four pentads earlier than that in 2006. Thus, a drought-induced ET reduction could be the reason for the WSO delay in 2006.

3.3. TES δD Suggested ET Reduction in 2006

TES δD observations also suggest ET reduction in 2006 relative to baseline years. Owing to the limited availability of TES observations in time, we study TES δD changes between 2006 and 2007, 2008, and 2009. Figure 3 shows the distribution of δD versus SPHU over these 4 years. The evaporation curves (i.e., the green and blue lines) are obtained from the theoretical model (Worden et al., 2007). The green lines represent mixing models, in which air from a dry and isotopically depleted source such as from the middle troposphere mixed with air from an ET (top green line) and oceanic (bottom green line) source. Similarly, the blue lines represent the "rainfall" curve describing how air parcels become more isotopically depleted and the air condenses at a temperature of ~277 K (Wright et al., 2017). Observations near the top green line can only come from an enriched source such as transpiration. Due to rain drop evaporation and convergence of depleted air parcels associated with deep convection, there are δD values below the bottom oceanic (blue) curve (i.e., the ocean Rayleigh curve); these values will not be discussed in this study. For both water vapor sources, SPHU is set to 20 g/kg, consistent with the relative humidity range of ~70–80% for typical daytime surface air temperatures during the southern Amazon transition season (Figure 3). According to Wright et al. (2017), if the free tropospheric moistening is dominated by upward mixing of local ET, then the larger SPHU in the free troposphere associated with higher values of δD (e.g., the red dots with SPHU values ~8 g/kg in Figure 3c) could be attributed to a land source. If the moistening were dominated by transport from oceanic sources, the larger SPHU would be associated with lower values of δD (e.g., the red dots with SPHU values ~8 g/kg in Figure 3a).

Here the results shows that the larger SPHU is associated with lower δD values in 2006 relative to the other 3 years during the late transition (Figure 3), suggesting a relatively smaller contribution from local ET in 2006. The TES δD spatial differences between these 3 years and 2006 also suggest lower δD values during the late transition of 2006 (Figure not shown). The regional mean δD value of 2006 is −135.8 ± 26.2‰, relatively lower than the values in 2007 (−124.8 ± 16.6‰), 2008 (−133.8 ± 20.3‰), and 2009 (−129.2 ± 19.5‰). The root-mean-square of the distribution is used as the error, since the data are effectively random at the monthly timescale (Worden et al., 2007). In the late transition of 2006, 2007, 2008, and 2009, ERA-Interim 500-hPa vertical velocities are 0.013, 0.016, 0.015, and 0.019 Pa/s, respectively, and the mean value during the late transition of 2001–2015 is 0.015 ± 0.003 Pa/s. Thus, the lower δD value in 2006 is not associated with strong subsidence-induced isotopic depletion, and the relative contribution of local ET to precipitation is reduced during the 2006 late transition.

4. Discussion

Several severe droughts and increasing DSL have been observed in Amazonia in the recent decades. The timing of WSO is an important proxy of Amazonian DSL. Fu et al. (2013) suggest that the increased DSL at a rate of 1.3 ± 0.5 pentads per decade since 1979 is mainly caused by the delay of WSO at a rate of 0.9 ± 0.4 pentads per decade. Thus, the 2006 three-pentad delay of WSO (Table S1) and the frequency at which similar delays occur are important to climate studies over Amazonia. Using the improved Priestley Taylor-JPL ET algorithm, Purdy et al. (2018) show that transpiration and canopy evaporation are the dominant ET components

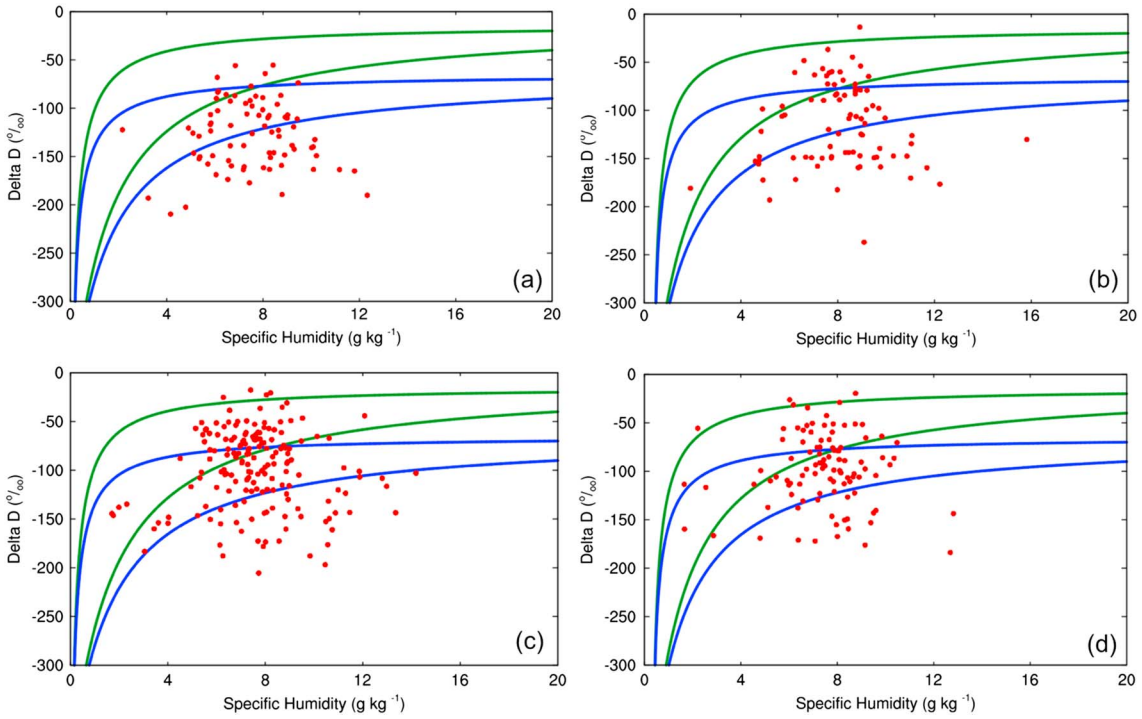

Figure 3. Tropospheric Emission Spectrometer observed deuterium content and specific humidity in the lower troposphere (825–600 hPa) during −6–0 pentad before the climatological wet season onset in (a) 2006, (b) 2007, (c) 2008, and (d) 2009 over 5–15°S, 55–70°W. The green lines and blue lines represent transpiration and oceanic sources, respectively. The red dots spread between the two solid green lines represent local evapotranspiration (q = 20 g/kg; $\delta D = -30‰$) and that spread between the two blue lines represent oceanic evaporation (q = 20 g/kg; $\delta D = -80‰$). This grouping method is statistical and cannot exactly separate water vapor from these two sources.

(up to ~80%) over Amazonia. Thus, with the 2005 drought-induced canopy biomass reduction and slow recovery, local ET reduction in subsequent years would be expected.

We acknowledge the uncertainties in the observational data sets used in this study; however, they do not affect our analyses and conclusions. In addition to TRMM precipitation, we use the Global Precipitation Climate Project (GPCP) product to identify WSO. Even though the WSO estimates from GPCP are different from those of TRMM (Table S6), our conclusions are robust against the choice of either TRMM or GPCP (Text S4). Here ET_{OBS} calculated from any of the GRACE TWS product shows similar variability between 2006 and the mean of the six baseline years (Table S5). We also quantify the ET_{OBS} uncertainty, which may be better constrained in future given further refinement of the retrieval technique (Tapley et al., 2004).

By using multiple observational data sets, this study quantitatively shows that the legacy of a drought is to reduce ET in subsequent seasons and delay the timing of WSO. This conclusion is consistent with the study of Wright et al. (2017), which shows that rainforest transpiration enables an increase of shallow convection, moistens the lower troposphere, and destabilizes the atmosphere during the initial stage of the dry-to-wet transition. This result is also indicative of the WSO dynamics at the scale of the broader Amazon forest. For example, the WSO in a larger region (0–15°S, 55–70°W), dominated by evergreen tropical trees (Figure S2a), also shows a delayed WSO in both 2005 and 2006 (Table S7). However, the WSO over 5–15°S, 50–70°W is only delayed in 2005 (Table S7), which could be associated with the reduced forest cover fraction (Figure S2b). We also investigate the 2010 drought in different Amazonian subregions but cannot find a single baseline case during 2001–2015 to identify the WSO delay associated with a drought legacy effect (Text S3). Nevertheless, ET_{OBS} anomaly value is −59 mm/year in 2011, suggesting an ET reduction after the 2010 drought (Figure S5).

Zemp et al. (2017) elaborate on a possible self-amplified Amazonian forest loss due to vegetation-atmosphere feedbacks. The case study we offer here using observations from multiple sources implies that forest legacy effect may extend the DSL and potentially cause more Amazonian forest loss, supporting the conclusion by

Zemp et al. (2017). This research shows that the study of other drought events (e.g., the 2015 drought; Figure S1c) is limited by the length of the observational record (e.g., TES δD), observational gaps (e.g., increased observational gaps of GRACE after 2010), and the inconsistency between basin-based observations and large-scale gridded observations. Thus, the long-term consistent deuterium retrievals from Atmospheric Infrared Sounder and the ET product from ECOsystem Spaceborne Thermal Radiometer Experiment on Space Station could provide important observational constraints to understand land-atmosphere feedback and therefore precipitation forecast.

5. Conclusions

In this study, both an observationally constrained ET product and TES δD suggest that a drought-disturbed canopy during 2005 led to reduced ET and a late dry-to-wet transition in 2006. Even though both ET_{OBS} and Q_{ATMO} reduction can be associated with a delayed WSO in Amazonia, observational evidence indicates that reduced ET in 2006 is the primary factor that triggered a three-pentad WSO delay (compared to the 2001–2015 mean) in 2006. Thus, the observation-based analyses support the hypothesis that forest loss can delay WSO through ET reduction. This study extends the time frame of drought memory discussed in previous research, and it underscores the importance of investigating drought memory effects on timescales of a year or longer.

Acknowledgments
Funding was provided by the NASA Carbon Cycle Science Program and the NASA Aqua and Terra Science Team program. The computations were performed at the NASA Ames Research Center. TRMM precipitation is at https://pmm.nasa.gov/data-access/downloads/trmm. TESHDO and SPHU are at https://avdc.gsfc.nasa.gov/index.php. GRACE data are available at http://grace.jpl.nasa.gov. PERSIANN precipitation is at https://www.ncei.noaa.gov/data/precipitation-persiann/access/. CRU precipitation is at https://crudata.uea.ac.uk/cru/data/hrg/cru_ts_4.02/cruts.1811131722.v4.02/pre/. The SO-HYBAM discharge measurements are at http://www.ore-hybam.org/. ERA-Interim is at https://rda.ucar.edu/. We appreciate Dr. George Huffman for providing valuable suggestions on TRMM precipitation, Dr. Sassan Saatchi for providing the QSCAT data, and Dr. Bin Zhao for providing suggestions on statistical methods. J. L., M. S., J. R. W., A. A. B., and S. W. carried out the research at JPL, Caltech, under a contract with NASA. M. S. also carried out the research at the Joint Institute for Regional Earth System Science and Engineering, UCLA.

References

Aragão, L. E. O. C., Poulter, B., Barlow, J. B., Anderson, L. O., Malhi, Y., Saatchi, S., et al. (2014). Environmental change and the carbon balance of Amazonian forests. *Biological Reviews*, *89*, 913–931. https://doi.org/10.1111/brv.12088

Ashouri, H., Hsu, K.-L., Sorooshian, S., & Braithwaite, D. K. (2015). PERSIANN-CDR: Daily precipitation climate data record from multisatellite observations for hydrological and climate studies. *Bulletin of the American Meteorological Society*, *96*, 69–83. https://doi.org/10.1175/BAMS-D-13-00068.1

Betts, R. A., Cox, P. M., Collins, M., Harris, P. P., Huntingford, C., & Jones, C. D. (2004). The role of ecosystem-atmosphere interactions in simulated Amazonian precipitation decrease and forest dieback under global climate warming. *Theoretical and Applied Climatology*, *78*(1-3), 157–175. https://doi.org/10.1007/s00704-004-0050-y

Brando, P. M., Balch, J. K., Nepstad, D. C., Morton, D. C., Putz, F. E., Coe, M. T., et al. (2014). Abrupt increases in Amazonian tree mortality due to drought–fire interactions. *Proceedings of the National Academy of Sciences*, *111*, 6347–6352. https://doi.org/10.1073/pnas.1305499111

Brown, D., Worden, J. R., & Noone, D. (2008). Comparison of atmospheric hydrology over convective continental regions using water vapor isotope measurements from space. *Journal of Geophysical Research*, *113*, D15124. https://doi.org/10.1029/2007JD009676

Dickinson, R. E., & Kennedy, P. (1992). Impacts on regional climate of Amazon deforestation. *Geophysical Research Letters*, *19*(19), 1947–1950. https://doi.org/10.1029/92GL01905

Duffy, P. B., Brando, P., Asner, G. P., & Field, C. B. (2015). Projections of future meteorological drought and wet periods in the Amazon. *Proceedings of the National Academy of Sciences*, *112*, 13,172–13,177. https://doi.org/10.1073/pnas.1421010112

Eltahir, E. A. B., & Bras, R. L. (1994). Precipitation recycling in the Amazon basin. *Quarterly Journal of the Royal Meteorological Society*, *120*(518), 861–880. https://doi.org/10.1256/smsqj.51805

Fu, R., Yin, L., Li, W., Arias, A., Dickinson, R. E., & Huang, L. (2013). Increased dry-season length over southern Amazonia in recent decades and its implication for future climate projection. *Proceedings of the National Academy of Sciences*, *110*, 18,110–18,115. https://doi.org/10.1073/pnas.1302584110

Galewsky, J., Larsen, H. S., Field, R. D., Worden, J. R., Risi, C., & Schneider, M. (2016). Stable isotopes in atmospheric water vapor and applications to the hydrologic cycle. *Reviews of Geophysics*, *54*, 809–865. https://doi.org/10.1002/2015RG000512

Gedney, N., & Valdes, P. J. (2000). The effect of Amazonian deforestation on the Northern Hemisphere circulation and climate. *Geophysical Research Letters*, *27*(19), 3053–3056. https://doi.org/10.1029/2000GL011794

Hirota, M., Holmgren, M., Van Nes, E. H., & Scheffer, M. (2011). Global resilience of tropical forest and savanna to critical transitions. *Science*, *334*, 232–235. https://doi.org/10.1126/science.1210657

Huffman, G. J., Bolvin, D. T., Nelkin, E. J., & Wolff, D. B. (2007). The TRMM multisatellite precipitation analysis (TMPA): Quasi-global, multiyear, combined-sensor precipitation estimates at fine scales. *Journal of Hydrometeorology*, *8*, 38–55. https://doi.org/10.1175/JHM560.1

Li, W., & Fu, R. (2004). Transition of the large-scale atmospheric and land surface conditions from the dry to the wet season over Amazonia as diagnosed by the ECMWF Re-Analysis. *Journal of Climate*, *17*, 2637–2651. https://doi.org/10.1175/1520-0442(2004)017<2637:TOTLAA>2.0.CO;2

Li, W., Fu, R., & Dickinson, R. E. (2006). Rainfall and its seasonality over the Amazon in the 21st century as assessed by the coupled models for the IPCC AR4. *Journal of Geophysical Research*, *111*, D02111. https://doi.org/10.1029/2005JD006355

Maeda, E. E., Ma, X., Wagner, F. H., Kim, H., Oki, T., Eamus, D., & Huete, A. (2017). Evapotranspiration seasonality across the Amazon Basin. *Earth System Dynamics*, *8*, 439–454. https://doi.org/10.5194/esd-8-439-2017

Malhi, Y., Roberts, J. T., Betts, R. A., Killeen, T. J., Li, W., & Nobre, C. A. (2008). Climate change, deforestation, and the fate of the Amazon. *Science*, *319*, 169–172. https://doi.org/10.1126/science.1146961

New, M., Hulme, M., & Jones, P. (2000). Representing twentieth-century space–time climate variability. Part II: Development of 1901–96 monthly grids of terrestrial surface climate. *Journal of Climate*, *13*(13), 2217–2238. https://doi.org/10.1175/1520-0442(2000)013<2217:RTCSTC>2.0.CO;2

Nobre, C. A., Sellers, P. J., & Shukla, J. (1991). Amazonian deforestation and regional climate change. *J. Climate*, *4*(10), 957–988. https://doi.org/10.1175/1520-0442(1991)004<0957:ADARCC>2.0.CO;2

Noone, D., Galewsky, J., Sharp, Z. D., Worden, J., Barnes, J., Baer, D., et al. (2011). Properties of air mass mixing and humidity in the subtropics from measurements of the D/H isotope ratio of water vapor at the Mauna Loa Observatory. *Journal of Geophysical Research*, *116*, D22113. https://doi.org/10.1029/2011JD015773

Oyama, M. D., & Nobre, C. A. (2003). A new climate-vegetation equilibrium state for Tropical South America. *Geophysical Research Letters*, *30*(23), 2199. https://doi.org/10.1029/2003GL018600

Poorter, L., Bongers, F., Aide, T. M., Almeyda, Zambrano, A. M., Balvanera, P., Becknell, J. M., et al. (2016). Biomass resilience of neotropical secondary forests. *Nature*, *530*, 211–214. https://doi.org/10.1038/nature16512

Purdy, A. J., Fisher, J. B., Goulden, M. L., Colliander, A., Halverson, G., Tu, K., & Famiglietti, J. S. (2018). SMAP soil moisture improves global PT-JPL evapotranspiration product. *Remote Sensing of Environment*, *219*, 1–14. https://doi.org/10.1016/j.rse.2018.09.023

Risi, C., Noone, D., Frankenberg, C., Worden, J. R., (2013). Role of continental recycling in intraseasonal variations of continentalmoisture as deduced from model simulations and water vapor isotopic measurements. *Water Resources Research*, *49*, 4136–4156. https://doi.org/10.1002/wrcr.20312

Rodell, M., Famiglietti, J. S., Chen, J., Seneviratne, S. I., Viterbo, P., Holl, S., Wilson, C. R., (2004). Basin scale estimates of evapotranspiration using GRACE and other observations. *Geophysical Research Letters*, *31*, L20504. https://doi.org/10.1029/2004GL020873

Saatchi, S., Asefi-Najafabady, S., Malhi, Y., Aragão, L. E. O. C., Anderson, L. O., Myneni, R. B., & Nemani, R. (2013). Persistent effects of a severe drought on Amazonian forest canopy. *Proceedings of the National Academy of Sciences*, *110*, 565–570. https://doi.org/10.1073/pnas.1204651110

Sakumura, C., Bettadpur, S., & Bruinsma, S. (2014). Ensemble prediction and intercomparison analysis of GRACE time-variable gravity field models. *Geophysical Research Letters*, *41*, 1389–1397. https://doi.org/10.1002/2013GL058632

Salati, E., & Vose, P. B. (1979). Amazon basin: A system in equilibrium. *Science*, *225*(4658), 129–138. https://doi.org/10.1126/science.225.4658.129

Shi, M., Liu, J., Zhao, M., Yu, Y., & Saatchi, S. (2017). Mechanistic processes controlling persistent changes of forest canopy structure after 2005 Amazon drought. *Journal of Geophysical Research: Biogeosciences*, *122*, 3378–3390. https://doi.org/10.1002/2017JG003966

Staver, A. C., Archibald, S., & Levin, S. A. (2011). The global extent and determinants of savanna and forest as alternative biome states. *Science*, *334*, 230–232. https://doi.org/10.1126/science.1210465

Swann, A. L. S., & Koven, C. D. (2017). A direct estimate of the seasonal cycle of evapotranspiration over the Amazon basin. *Journal of Hydrometeorology*, *18*, 2173–2185. https://doi.org/10.1175/JHM-D-17-0004.1

Tapley, B. D., Bettadpur, S., Ries, J. C., Thompson, P. F., & Watkins, M. M. (2004). GRACE measurements of mass variability in the Earth system. *Science*, *305*(5683), 503–505. https://doi.org/10.1126/science.1099192

Verbesselt, J., Umlauf, N., Hirota, M., Holmgren, M., Van Nes, E. H., Herold, M., et al. (2016). Remotely sensed resilience of tropical forests. *Nature Climate Change*, *6*, 1028–1031. https://doi.org/10.1038/nclimate3108

Wong, S., Del Genio, A. D., Wang, T., Kahn, B., Fetzer, E. J., & L'Ecuyer, T. S. (2016). Responses of tropical ocean clouds and precipitation to the large-scale circulation: Atmospheric water budget-related phase space and dynamical regimes. *Journal of Climate*, *29*, 7127–7143. https://doi.org/10.1175/JCLI-D-15-0712.1

Worden, J. R., Bowman, K., Noone, D., Beer, R., Clough, S., Eldering, A., et al. (2006). Tropospheric Emission Spectrometer observations of the tropospheric HDO/H_2O ratio: Estimation approach and characterization. *Journal of Geophysical Research*, *111*, D16309. https://doi.org/10.1029/2005JD006606

Worden, J. R., Noone, D., & Bowman, K. W. (2007). Importance of rain evaporation and continental convection in the tropical water cycle. *Nature*, *445*, 528–532. https://doi.org/10.1038/nature05508

Wright, J. S., Fu, R., Worden, J. R., Chakraborty, S., Clinton, N. E., Risi, C., et al. (2017). Rainforest-initiated wet season onset over the southern Amazon. *Proceedings of the National Academy of Sciences*, *114*, 8481–8486. https://doi.org/10.1073/pnas.1621516114

Xu, C., Hantson, S., Holmgren, M., Nes, E. H., Staal, A., & Scheffer, M. (2016). Remotely sensed canopy height reveals three pantropical ecosystem states. *Ecology*, *97*, 2518–2521. https://doi.org/10.1002/ecy.1470

Zemp, D. C., Schleussner, C.-F., Barbosa, H. M., Marina, H., Montade, V., Sampaio, G., et al. (2017). Self-amplified Amazon forest loss due to vegetation-atmosphere feedbacks. *Nature Communications*, *8*, 14681. https://doi.org/10.1038/ncomms14681

References From the Supporting Information

AghaKouchak, A., Nasrollahi, N., & Habib, E. (2009). Accounting for uncertainties of the TRMM satellite estimates. *Remote Sensing*, *1*, 606–619. https://doi.org/10.3390/rs1030606

Habib, E., & Krajewski, W. F. (2001). Uncertainty analysis of the TRMM ground-validation radar-rainfall products: Application to the TEFLUN-B field campaign. *Journal of Applied Meteorology*, *41*(5), 558–572. https://doi.org/10.1175/1520-0450(2002)041<0558:UAOTTG>2.0.CO;2

Landerer, F. W., & Swenson, S. C. (2012). Accuracy of scaled GRACE terrestrial water storage estimates. *Water Resources Research*, *48*, W04531. https://doi.org/10.1029/2011WR011453

Wong, S., & Behrangi, A. (2018). Regime-dependent differences in surface freshwater exchange estimates over the ocean. *Geophysical Research Letters*, *45*, 955–963. https://doi.org/10.1002/2017GL075567